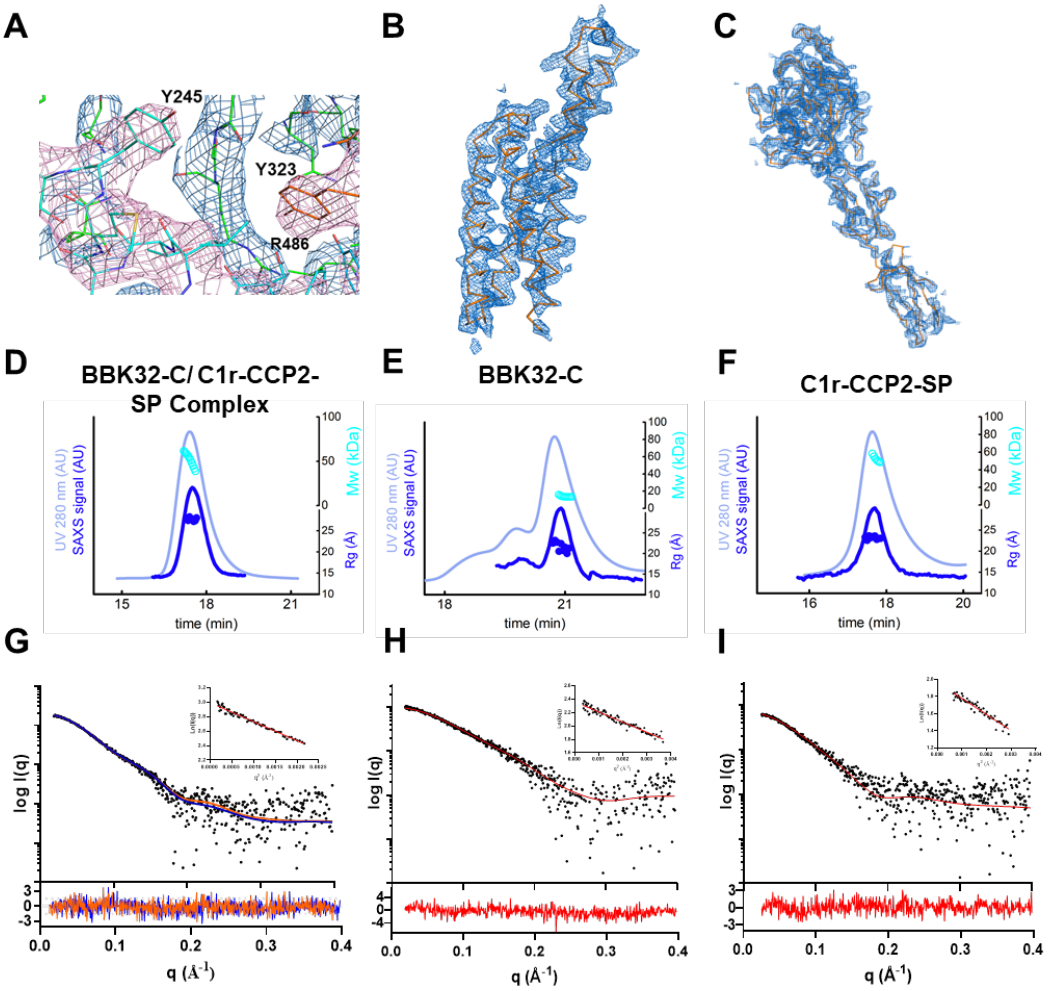

Supplementary Figure S1. X-ray crystallography and SEC-SAXS data. 2*Fo-Fc* density contoured at 1.2 σ for **A)** Close-up view of representative area of the BBK32-C/C1r interface. **B)** BBK32-C (Chain: I) and **C)** C1r (Chains: A, B). **D-F)** SEC-MALS-SAXS chromatographs for BBK32-C/C1r-CCP2-SP, BBK32-C, and C1r-CCP2-SP. Solid lines represent the UV 280 nm (light blue) or integrated SAXS signal (dark blue) in arbitrary units, while symbols represent molecular mass (cyan) and Rg values for each collected SAXS frame (blue) versus elution time. **G)** Experimental SAXS curve for the C1r-CCP2-SP/BBK32-C complex sample (black) shown with calculated theoretical SAXS of the model (orange). The co-crystal of BBK32-C in complex with an autoproteolytic fragment of human C1r (PDB: 7MZT) where the CCP1 domain was removed was compared to the SAXS theoretical model curve obtained for the BBK32-C/C1r-CCP2-SP using FoXS. The calculated fit is shown in blue (χ^2 = 1.20). **H-I)** Experimental SAXS curves for BBK32-C and C1r-CCP2-SP (black), respectively with FoXS calculated model curves (red). Residual error plots are presented below with Guinier plots (inset) for all SAXS curves.

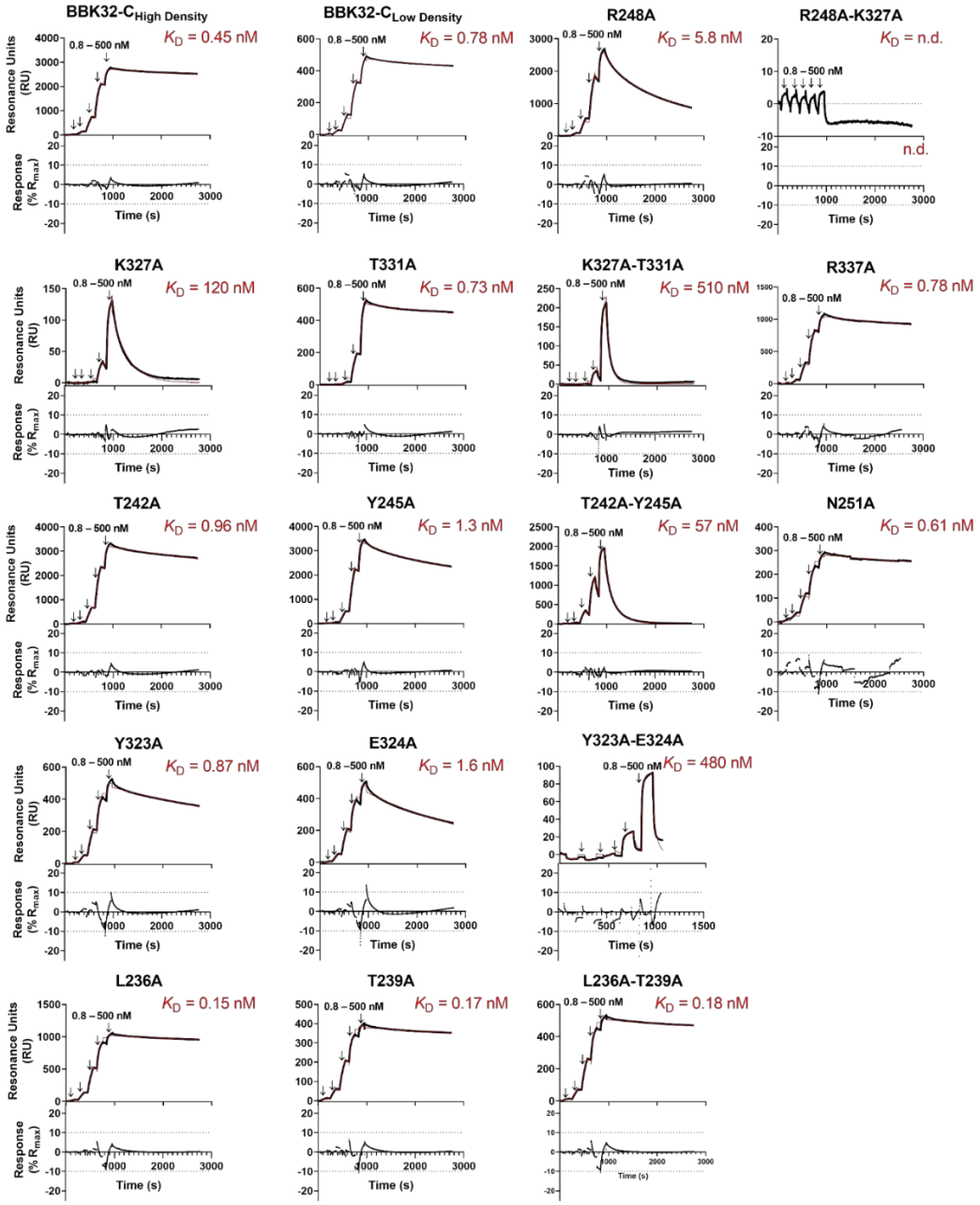

Supplemental Figure S2. Kinetic fits of SPR binding assays with BBK32-C site-directed mutants. Fitted sensorgrams of each curve presented in **Fig. 2C** with experimental data (black) and a 1:1 Langmuir model fit (red). Downward arrows indicate injection phases of each C1r-CCP2-SP concentration in the series (0.8, 4.0, 20.0, 100, 500 nM). Residual plots for each SPR curve is normalized as a function of the fitted R_{max} (**Table 3**). Dissociation constants (K_D) are shown as an average of duplicate experimentation. Additional SPR parameters for these experiments are shown in **Table 3.** Resulting curves were unable to be fit for BBK32-R248A-K327A and therefore do not include K_D nor resulting residual plot. Additional SPR parameters for these curves are presented in **Table 3**.

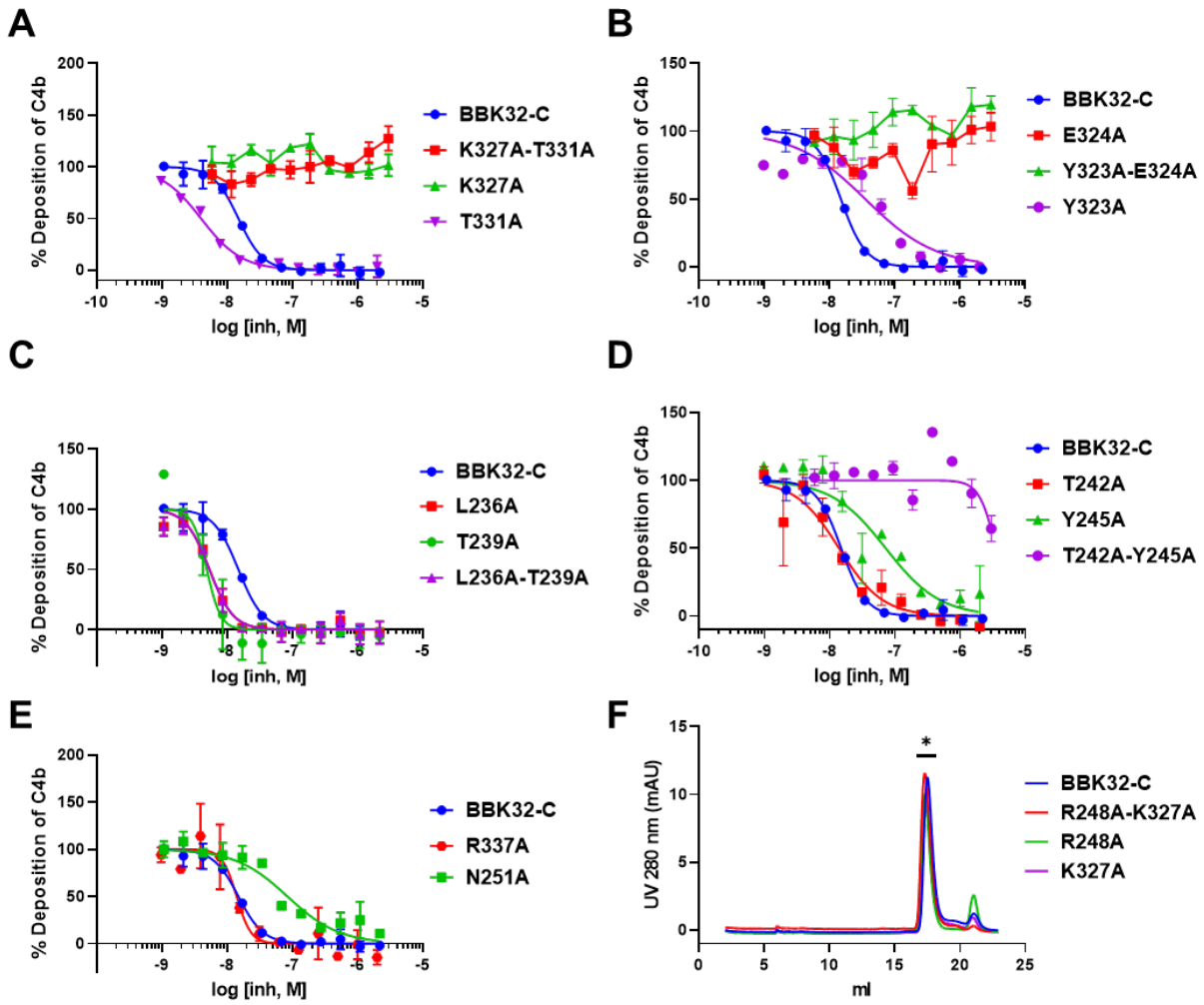

Supplemental Figure S3. Complement inhibitory activity and gel filtration data for additional BBK32-C site-directed mutants. Classical pathway ELISAs were performed to determine the ability of BBK32-C mutants to inhibit the classical pathway of complement in vitro. IC_{50} and 95% confidence intervals are shown in **Table 3**. BBK32-C is shown on each plot for comparison only and is replotted from the BBK32-C data shown in **Fig. 4A**. **F)** Gel filtration analysis on a Superdex 200 Increase 10/300 GL shows monodisperse peaks of similar elution volumes, indicating similar tertiary structure of BBK32-C mutants compared to wild type. Single peaks for BBK32-C and site-directed mutants between 17.3 and 17.5 mLs were observed (denoted with *).

Table S1. Strains, plasmid constructs, and oligonucleotides used in this study.

***E. coli* strains**		
NEB® 5-alpha	*fhuA2* (*argF-lacZ*)U169 *phoA glnV44* 80(*lacZ*)ΔM15 *gyrA96 recA1 relA1 endA1 thi-1 hsdR17*	New England Biolabs
***B. burgdorferi* strains**		
B314	Serum-sensitive, non-infectious *B. burgdorferi* B31 derivative strain lacking all linear plasmids	*(56)*
B314 pBBE22*luc*	Serum-sensitive, non-infectious *B. burgdorferi* B31 derivative strain lacking all linear plasmids; shuttle vector encodes *bbe22* and *B. burgdorferi* codon optimized *luc* gene under the control of a strong borrelial promoter (P_{flaB}-*luc*).	*(74)*
B314 pCD100	Serum-sensitive, non-infectious *B. burgdorferi* B31 derivative strain lacking all linear plasmids with wildtype *bbk32* under control of its native promoter in pBBE22*luc*.	This study
B314 pAP5	Serum-sensitive, non-infectious *B. burgdorferi* B31 derivative strain lacking all linear plasmids with *bbk32* R248A under control of the *bbk32* promoter in pBBE22*luc.*	This study
B314 pAP6	Serum-sensitive, non-infectious *B. burgdorferi* B31 derivative strain lacking all linear plasmids with *bbk32* K327A under control of the *bbk32* promoter in pBBE22*luc*.	This study
B314 pAP7	Serum-sensitive, non-infectious *B. burgdorferi* B31 derivative strain lacking all linear plasmids with *bbk32* R248A/K327A under control of the *bbk32* promoter in pBBE22*luc*.	This study
Plasmids		
pBBE22*luc*	Borrelial shuttle vector containing *bbe22* and *B. burgdorferi* codon-optimized *luc* gene under the control of a strong borrelial promoter (P_{flaB}-*luc*)	*(74)*
pCD100	Knock in construct of wild-type BBK32 with its native promoter in pBBE22*luc*.	*(33)*
pAP5	Knock in construct encoding BBK32 R248A under the control of its native *bbk32* promoter in pBBE22*luc*.	This study
pAP6	Knock in construct encoding BBK32 K327A under the control of its native BBK32 promoter in pBBE22*luc*.	This study
pAP7	Knock in construct encoding BBK32 R248A-K327A under the control of its native BBK32 promoter in pBBE22*luc*.	This study

Oligonucleotides			
R248A mutant F	GTATTCTACAGCACTTGACAACTTTGCTAAAGCC	Oligonucleotide pair used for site-directed mutagenesis of *bbk32* R248 for conversion to alanine and generate pAP5	This study
R248A mutant R	AGTTGTCAAGTGCTGTAGAATACATTTGGGTTAGCTTTGT		
pncAF	TATTGGAATTAATAGGCGGTGATG	Oligonucleotide pair used to confirm *bbk32* knock-in constructs	*(41)*
lucF	GAGGGGTTGTATTTGTTGACG		
K327A frag F	AAGTAAGTGTAAAGACTGCAGCAAATTTTGTATACATA	Oligonucleotide pair used to amplify the *bbk32* K327A fragment for recombination with either pCD100 (to make pAP6) or pAP5 (to make pAP7).	This study
K327A frag R	TATGTATACAAAATTTGCTGCAGTCTTTACACTTACTT		
backbone frag F	GGCTACATAATATGTCGACCTGCAGGCATGCAAGCTT	Oligonucleotide pair used to amplify either pCD100 (to make pAP6) or pAP5 (to make pAP7) fragments for recombination with the K327A fragment.	This study
backbone frag R	AAGCTTGCATGCCTGCAGGTCGACATATTATGTAGCC		